Journal of Chemical and Petroleum Engineering (JChPE)
Print ISSN: 2423-673X Online ISSN: 2423-6721

Prediction of Bubble Point Pressure Using New Hybrid Computational Intelligence Models

Mohammad Naveshki, Ali Naghiei, Pezhman Soltani Tehrani, Mehdi Ahmadi Alvar, Hamzeh Ghorbani *, Nima Mohamadian, Jamshid Moghadasi *

1. Department of Petroleum Engineering, Sahand University of Technology, Tabriz, Iran. E-mail: m.naveshki@gmail.com
2. Faculty of Engineering, University of Garmsar, Garmsar, Iran. E-mail: alinaghiei@gmail.com
3. Department of Petroleum Engineering, Kish International Campus, University of Tehran, Kish, Iran. E-mail: p.soltani.tehrani@ut.ac.ir
4. Faculty of Engineering, Department of computer Engineering, Shahid Chamran University, Ahwaz, Iran. E-mail: m-ahmadialvar@stu.scu.ac.ir
5. Young Researchers and Elite Club, Islamic Azad University, Ahvaz, Iran. E-mail: hamzehghorbani68@yahoo.com
6. Young Researchers and Elite Club, Islamic Azad University, Omidiyeh, Iran. E-mail: nima.0691@gmail.com
7. Department of Petroleum Engineering, Petroleum Industry University, Ahvaz, Iran. E-mail: j.moghadasi@put.ac.ir

ARTICLE INFO

Article History:
Received: 03 December 2020
Revised: 08 May 2021
Accepted: 10 May 2021

Article type: Research

Keywords:
Bubble Point Pressure Prediction,
DWKNN-GSA,
DWKNN-ICA,
Hybrid Computational Intelligence,
Machine Learning

ABSTRACT

Determining BPP is one of the critical parameters for developing oil and gas reservoirs, and has this parameter requires a lot of time and money.. As a result, this study aims to develop a new predictive model for BPP that uses some available input variables such as solution oil ratio (R_s), gas specific gravity (γ_g), API Gravity (API). In this study, two innovatively combined hybrid algorithms, DWKNN-GSA and DWKNN-ICA, are developed to predict BPP. The study outcomes show the models developed are capable of predicting BPP with promising performance, where the best result was achieved for DWKNN-ICA (RMSE = 0.90276 psi and R^2 = 1.000 for the test dataset). Moreover, the performance comparison of the developed hybrid models with some previously developed models revealed that the DWKNN-ICA outperforms the former empirical models concerning perdition accuracy. In addition to presenting new techniques in the present study, the effect of each of the input parameters on BPP was evaluated using Spearman's correlation coefficient, where the API and Rs have the lowest and the highest impact on the BPP.

Introduction

The phase behavior and volumetric changes of reservoir fluids, typically multiphase, are a function of the pressure and temperature of the reservoir and the composition of fluid. During the petroleum recovery period, the temperature of the reservoir is often maintained at an approximately constant value. Bubble point pressure (BPP) is the pressure at which the first gas bubble appears at a certain temperature [1], that is regarded as one of the critical parameters in reservoir engineering since it is used to assess the basic parameters of the reservoir necessary

* Corresponding author: H. Ghorbani (Email address: hamzehghorbani68@yahoo.com)
* Corresponding author: J. Moghdasi (Email address j.moghadasi@put.ac.ir)
Journal of Chemical and Petroleum Engineering, 2021, 55(2): 203- 222.
Publisher: University of Tehran, College of Engineering *DOI: 10.22059/jchpe.2021.314719.1341*

for development, completion and optimization of oil and gas fields [2-6]. This property can be obtained in two ways: a) using experiments and sampling from bottom hole, b) or through experimental equations where the information related to these equations is gathered from field data [7]. Reservoir properties can be obtained through laboratory tests using the PVT test, which in turn is time-consuming, costly, and also the necessary conditions for this must be provided. For this reason, to avoid the cost and time-consuming nature of these laboratory tests, field data are used to predict bubble point pressure because these field data are taken routinely, quickly, and cheaply. However, Laboratory devices and conditions are not always available (sampling for testing and PVT test) [8]. Due to the great importance of developing and completing oil and gas fields, one of the tasks that have been done in recent years is applying field data to calculate and predict, as well as to determine the parameters used in the oil and gas industry, for example in The following areas have been addressed: reservoirs [9]; formation damage [10], wellbore stability [11], rheology and filtration [12], production [13-15]; drilling fluid [16-20], nano clay [21], well blowout [22], carbon dioxide-nitrogen gas mixtures [23-30].

Literature Review

In the oil and gas industry, predictions are made to obtain valuable information using a large amount of routine data, primarily to obtain the properties of oil and gas fluids. Some researchers have also used a series of equations derived from the equation of state (EOS) to get this valuable information [31-33].

Due to the high importance of PVT determination from 1940 onwards, many researchers have begun to predict and determine many equations. First in 1947, Standing [34] established two correlations to predict oil formation volume factor (OFVF) and BPP with input data parameters temperature (T), solution gas-oil ratio (R_s), gas specific gravity (γ_g) and oil density (API) which were obtained using the laboratory analyzes carried out on 105 Data set from 22 different samples of crude oils obtained from California.

Then, in 1980 Glaso [35] used 45 oil samples from the North Sea region to predict correlations to determine BPP and several other parameters (OFVF, R_s, and dead oil viscosity (μ_{OD})) where an average error of 20.43% was reported for BPP prediction. In 1988 Al-Marhoun [36] proposed two correlations for predicting BPP and OFVF. He used Middle Eastern crude oil using 160 data records from oilfields across the region.

In 1992, Dokla and Osman [37] presented an equation based on Al-Marhoun equations using 51 UAE crude oil test data to predict BPP. a year later, in 1993, Macary and El-Batanoney [3] provided equations for the BPP prediction, using previously proposed by Saleh et al. [38], Petrosky and Farshad [38] presented some equations for predicting BPP, Rs, and OFVF using 90 well-test data records from the Gulf of Mexico (U.S.A.). All the above-mentioned experimental equations are reported in detail, and the publication date and the number of data used in Table 1.

In recent years, many researchers have applied artificial intelligence to predict desired parameters in the different sectors of the oil and gas industry [39, 40].

Studies have shown that the accuracy of empirical equations for crude oils in a region is low, but crude oils of different geographical areas with different compositions may not be accurately predicted by empirical correlations and cause a substantial error [41, 42]. As a powerful tool, artificial intelligence have been widely used for forecasting PVT and other parameters in various sectors of oil and gas industry. For instance, in 1999, Gharbi et al. [43] using 5200 laboratory PVT analysis on 350 different crude oils using artificial neural network (ANN) model with error rate APD = -2.13%, AAPD = 6.48%, SD = 7.81 and R^2 = 0.9891.

In 1999, 2002 and 2003 Boukadi et al. [44], Al-Marhoun & Osman [45] and Goda et al. [35] using 92, 282 and 160 data for predicted BPP using artificial neural network (ANN) model was used where the error rate of APD% = 645, -0.2215, -0.0078, AAPD% = 6.50, 5.8915, 0.03070, SD = -, 8.6781, - and R^2 = 0.99, -, 0.9981 of region Oman, Saudi and Middle East. Rafiee-Taghanaki et al. [46] used the ANN and LSSVM methods to establish a mopdel for BPP prediction, where the best results showed APD = -0.36%, AAPD = 5.06%, RMSE = 146.62, and R^2 = 0.98.

In 2013, Salehinia et al. [47] used the NARX-HW, ANFIS-GP, and ANFIS-FCM methods for training the BPP prediction model using 755 data collected from Iran. Their best results presented APD = -0.97%, AAPD = 15.06% and R^2 = 0.94. Seyyedattar et al. [48], utilized LSSVM-CSA and ANFIS methods for establishing a prediction model for BPP using ; where the best results reported displayed APD = -0.267%, AAPD = 0.917% and R2 = 0.9962. most recently, in 2020, 79 data collected from Iran was used by Ghorbani et al. [49] for developing some BPP prediction models by employing different methods, including MLP, RBF-GA, CHPSO-ANFIS, and LSSVM methods. Where the CHPSO-ANFIS model showed the best result that included APD = 0.846, SD = 0.0126, for RMSE = 43.21 and R2 = 0.9902.

Table 1. Empirical correlations used to predict bubble point pressure (BPP) [49-51]

Author	Date	Origin	Error parameter	Data No.	Correlation
Standing [34]	1947	California	APD% = 4.8	105	$P_b = a1 * \left[\left(\frac{R_s}{\gamma_g}\right)^{a2} * 10^{a3*T-a4*API} - a5\right]$ a1=18.2, a2=0.83, a3=0.00091, a4=0.0125, a5=1.4
Glaso [35]	1980	North Sea	APD% = 1.8 SD = 6.98	41	$P_b = 10^{a1+a2*\log(G)-a3(\log(G))^2}$ $G = \left(\frac{R_s}{\gamma_g}\right)^{a4} * T^{a5} * API^{a6}$ a1=1.7669, a2=1.7447, a3=0.3021, a4=0.86, a5=0.172, a6=-0.989
Al-Marhoun [36]	1988	Middle East	APD% = -0.01 SD = 1.18	160	$P_b = a1 * R_s^{a2} * \gamma_g^{a3} * \gamma_o^{a4} * (T + 460)^{a5}$ a1=0.00538, a2=0.715082, a3=-1.8774, a4=3.1432, a5=1.326
Dokla & Osman [37]	1992	UAE	APD% = 0.45 SD = 10.37	51	$P_b = a1 * R_s^{a2} * \gamma_g^{a3} * \gamma_o^{a4} * (T + 460)^{a5}$ a1=0.83638E4, a2=0.724047, a3=-1.01049, a4=0.107791, a5=-0.95258
Macary & El-Batanony [3]	1993	Gulf of Suez	APD% = 7.04	90	$P_b = a1K[R_s^{a2} - a3]$ $K = EXP[a4T - a5\gamma_o - a6\gamma_g]$ a1=204.257, a2=0.51, a3=4.7927, a4=0.00077, a5=0.0097, a6=0.4003
Petrosky & Farshad [38]	1993	Gulf of Mexico	APD% = -0.17 SD = 2.56	90	$P_b = a1 * \left[{R_s}^{a2} / {\gamma_g}^{a3} * 10^X - a4\right]$ $X = a5 * T^{a6} * a7API^{a8}$ a1=112.727, a2=0.5774, a3=0.8439, a4=12.340, a5=4.561e-5, a6=1.3911, a7=7.916e-4, a8=1.5410

In this study, two hybrid models, DWKNN-ICA and DWKNN-GSA, were developed for BPP prediction by innovatively combining the DWKNN with two optimization algorithms, the ICA and GSA. To evaluate the accuracy performance of two hybrid models developed, the computational error for the DWKNN-ICA and DWKNN-GSA in BPP prediction was compared to those of five previously established artificial-intelligence-based empirical models. The results obtained demonstrate that the DWKNN-ICA and DWKNN-GSA can predict the BPP with significantly high accuracy that was much higher than those of the other previously proposed empirical models listed in Table 1. To authors' best knowledge, the developed hybrid models in the present study have not been applied for BPP prediction so far. The impressive performance and accuracy observed for the DW KNN-ICA and DW KNN-GSA models in BPP prediction suggest potential employment for prediction of other parameters.

Methodology

Work Flow

A quick and eye-catching view of the whole article is one of the best and most important methods for readers to present using workflow (Fig. 1). In this method, in order to determine the minimum and maximum, data must be normalized and then presented for input to the network (Eq. 1). Fig. 1, with a quick overview of the workflow for the paper presented in this study is that, 70% of the data were used for training and 30% of the data for testing in this study. To optimize the prediction, inputs were used to find better outputs from machine learning and deep learning. To avoid data range biases in the calculations, the variable values of all data records are normalized to a scale between -1 and +1 for their entire dataset distributions applying Eq. 1.

$$x_i^l = \left(\frac{x_i^l - xmin^l}{xmax^l - xmin^l}\right) * 2 - 1 \tag{1}$$

where x_i^l represents the value of attribute l of data record i, $xmin^l$ and $xmax^l$ are the minimum and maximum values of the attribute l among all the data records.

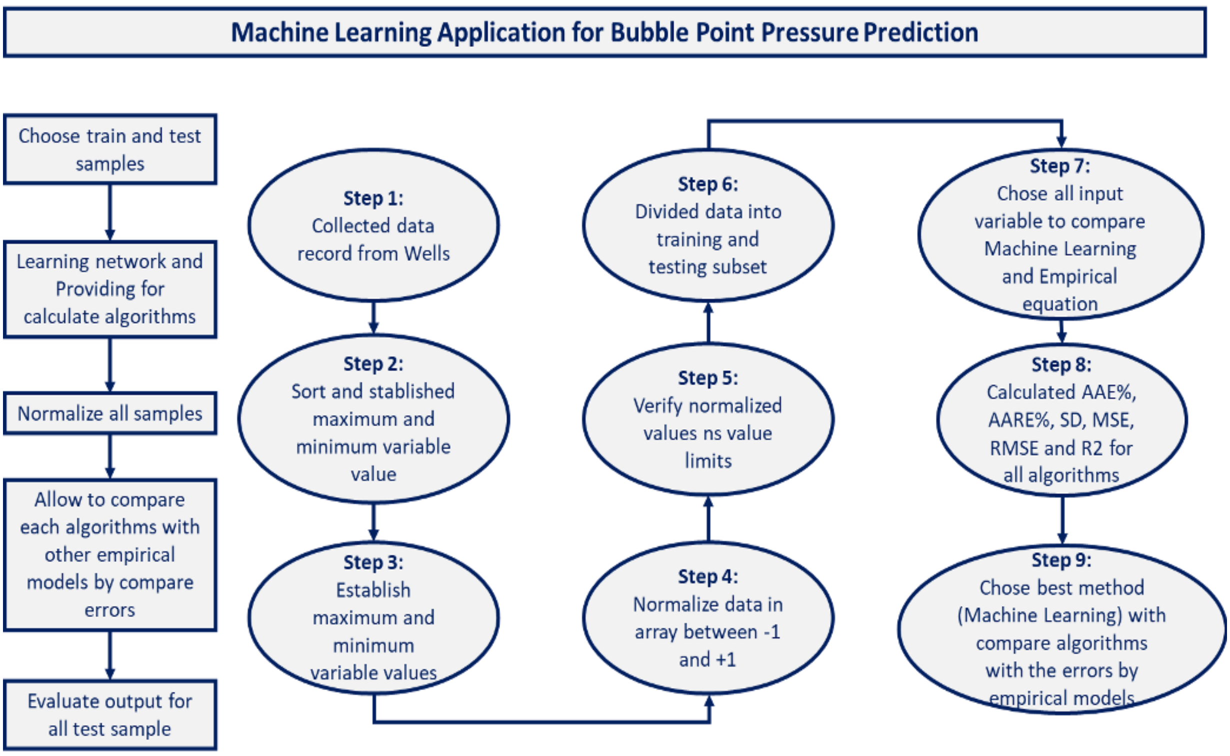

Fig. 1. Schematic diagram of the workflow sequence applied for comparing the prediction performance of machine learning algorithms and empirical models

Machine Learning Algorithm

Today, artificial intelligence is rooted in various industries and sciences and has found several of applications in various fields. The oil and gas industry has long been the focus of the whole world, and the reason is that the extracted oil and gas have changed the world. Many people did much work to optimize and find important and key parameters in the oil and gas industry, including: reservoir characterization [9, 49, 52]; production characterization [53-57]; drilling characterization [58-61]; fluid processing [62-64].

Artificial Neural Network

Distance-Weighted K-nearest Neighbor (DWKNN) algorithm

K-nearest neighbor (KNN) non-parametric, well-constructed, and data mining algorithm, which is known to be simply implemented [65]. This algorithm, a supervised method of machine learning, finds a group of K samples in the training subset closest to the testing sample than all training data in the data record, and calculates the average value of this K sample, and considers it as the estimated value. Three key points of this method are: i) a set of samples with labeled output data ii) a similarity or distance unit for calculating the distance between two samples iii) a K value to determine the number of neighborhoods. In DWKNN algorithm, for each testing sample, each sample of K set, based on how far it is from the testing sample, is given as a coefficient for the sample, so that if Indeed, this coefficient determines the magnitude of influence of the sample on the prediction output, farther samples have less influence on the output while closest samples have the greatest impact [66]. First, the distance between the test sample and all the training samples is calculated using Eq. (2).

$$D_i = \left(\sum_{j=1}^{M} \left|X_{ij} - X_j\right|^2\right)^{1/2} \quad , \qquad i = 1,2,\dots,N \tag{2}$$

where D_i is the Euclidean distance between the test sample and training sample, M stands for the number of features, N is the number of samples, X_{ij} and X_j are the training and testing samples, respectively. Then, K number sample of the training subset that has the lowest D_i values are chosen for estimating the value of dependent variable value for test data record X, using Eq. 3.

$$C_p = \frac{1}{K}\sum_{t=1}^{K} C_t \tag{3}$$

where C_p stands for the dependent variable predicted value for the testing data record, C_t represents the values of the dependent variable for the t^{th} nearest neighbor, and K is the number of identified nearest neighbors. Eq. 2 is used for KNN method, while in WKNN method, a weight is assigned to the dependent variable value of the nearest neighbor according to Eq. 4.

$$w_i = \frac{1/D_i}{\sum_{j=1}^{k}\left(1/D_i\right)} \quad , \qquad i = 1,2,\dots,K \tag{4}$$

where w_i represents the weight variable of the dependent variable to be excreted for i^{th} nearest neighbor using Eq. 5.

$$\mathrm{C_{un}} = \sum_{\mathrm{i=1}}^{\mathrm{k}} \mathrm{w_i C_i} \tag{5}$$

Optimization Algorithms

In this study, gravitational search algorithm and imperialist competitive algorithm, which are considered two evolutionary optimization algorithms capable of efficiently searching for convincible solution space, are employed to enhance the prediction performance.

Gravitational Search Algorithm (GSA)

In 2009, the GSA algorithm was proposed by Rashedi et al. [67] as a novel algorithm based on gravity laws. This algorithm considers the agents as objects that have masses. The agents are attracted to each other through gravitational force. The quality of attraction is directly related to gravity force, where the stronger the gravity results in, the greater quality [68]. In other words, the objects with more massive masses represent a stronger positional solution than those of lighter objects. As a result, the agent's position with a heavier mass is regarded as the optimal solution space. The fully detailed calculation steps for GSA employment is described by [69].

Imperialist Competitive Algorithm (ICA)

ICA is a population-based optimization algorithm that is inspired by colonial competition. In this algorithm, each population's individual constitutes a country; some countries are chosen as best countries or imperialists and others as poor or colonial countries [70]. The countries of the population are indeed possible solutions to the problem. Imperialist countries attract the colonial ones by applying assimilation policy in the direction of different optimization axes. Imperialist competition along with assimilation policy form the core of the ICA algorithm. This algorithm converges towards an optimal solution for its objective function) is through evolving by several iterations. The objective function applied is typically mean square error (MSE) to avoid getting trapped in local minima. The details of calculation step for employing GSA are described by Abdi et al. [71].

Hybrid Machine learning optimization algorithms

Two hybrid-optimizer machine learning models were developed and analyzed in this study, which are GSA-DWKNN is ICA-DWKNN. Since all the features do not equally influence the final solution, a weight coefficient was assigned to each feature to improve the perdition accuracy, and these weights were optimized using the optimization algorithms. The flowchart that describes the steps of generic implementation for the hybrid optimizer-DWKNN models is shown in Fig. 2.

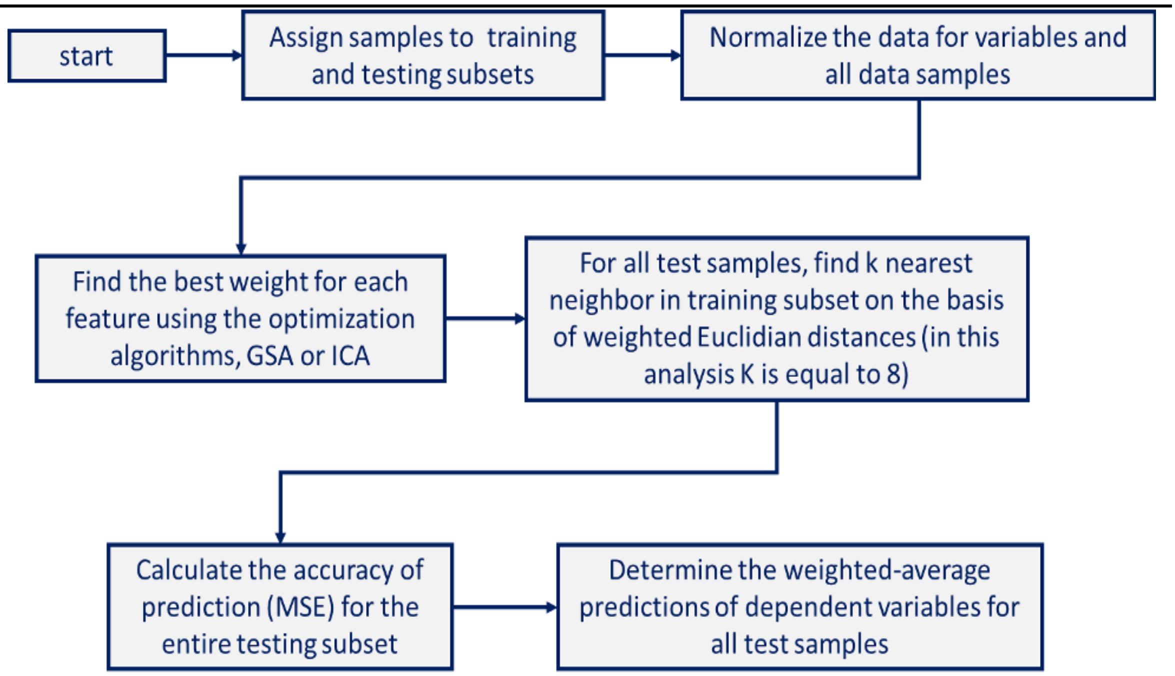

Fig. 2. Flow diagram of required implementations steps for the developed hybrid-optimizer machine learning models

The implementation steps of the hybrid-optimizer machine learning models involving are described in the following.

- Selection of the testing and training samples

First, to assess the performance of the model, the data records were divided into two subsets, testing and training subsets. In the KNN method, the selection of the training data is important; the more general the selected data, the more the model's prediction accuracy. As a result, the training samples were selected so that the selected training subset has a promising uniformity in terms of the distance between the data records.

- Normalization of all data records

Since each of the features (inputs) to the models may have ranged between different numbers, this reneges difference could have a negative effect on the distance criteria that may result in a considerable reduction of the model accuracy. To overcome that difficulty, normalization was employed as a proper solution. The data were normalized by transferring all the features into the fixed two reneges between 0 and 1 and 1 to -1 applying Eq. 6.

$$x_i^l = \left(\frac{x_i^l - xmin^l}{xmin^l - xmax^l}\right) * 2 - 1 \tag{6}$$

where x_i^l represents l^{th} feature value of i^{th} sample, $xmin^l$ and $xmax^l$stand for the minimum and the maximum values of the l^{th} feature in the whole data set.

- Finding the best weights for the features using GSA or ICA optimization algorithms

First, the distance equation is defined as Eq. 7.

$$D_i = \left(\sum_{j=1}^{M} wf_j \left|X_{ij} - X_j\right|^2\right)^{1/2} \quad , \qquad i = 1,2, \dots , N \tag{7}$$

Eq. 7 resulted in a new vector, W, that measures the influence of the features on the final distance value (see Eq. 8). Then, the optimal values of the weights' vectors were calculated using the optimization algorithms.

- Finding the nearest neighbor K for all testing data records

Once the optimal weights' vectors were calculated, K nearest neighbor in all the training samples was determined using the trial and error method for each testing data record. In this analysis, the best results were achieved when K was assigned to be 8.

- Determination of weighted predictions for all the testing data

For each test data record, the weighted predictions were made based on nearest neighbor k, applying Eqs. 4 and 5.

Finally, the prediction accuracy for both models, GSA-DWKNN and ICA-DWKNN, was calculated, applying MSE (see Eq. 8).

$$percent = 100 - \sum_{i=1}^{N} \frac{|\hat{y}_i - y_i|}{|y_i|} * 100 \tag{8}$$

where $\hat{y}_i$ and y_i stand for the predicted and the measured values of i^{th} testing data records.

Tables 2 and 3 list the value of applied control parameters used in the machine learning and optimizer algorithms. These values were determined by trial and errors for the analyzed dataset.

Table 2. DWKNN-GSA algorithm parameters.

GSA parameter's control	Value	DWKNN algorithm	Value
Euclidean distance adjustment factor	0.1	K-value (number of nearest neighbor)	8
Gravitational alpha exponent	2		
Maximum number of iterations	100		
Number of initial k-best agent used	3		
Population size	50		
Initial gravitational constant	10		

Table 3. DWKNN -ICA algorithm parameters

ICA parameter's control	Value	DWKNN algorithm	Value
Selection pressure	1	K-value (number of nearest neighbor)	8
Revolution rate	0.1		
Colonies mean cost coefficient	0.2		
Number of empires/imperialists	10		
Maximum number of iterations	100		
Revolution probability	0.05		
Assimilation coefficient	1.5		
Population size	50		

Data Collection & Data Analysis

In this study, a data set, a mixture of data samples from different parts of the world, was used to determine an optimal model for BPP. The parameters that affect the determination of BPP are temperature (*T*), solution gas-oil ratio (R_s), gas specific gravity (γ_g), and API. Table 4 summarizes the statistical distributions of these four data variables for the 567 data records compiled, where 398 records were used for training the model and 169 records were used for testing.

Table 4. Data record statistical characterization of the variables in this study

Parameters		Temperature	Solution gas oil ratio	Gas specific gravity	API	Bubble point pressure
Units		(F)	SCF/STB	-	-	psi
N	Valid	567	567	567	567	567
	Missing	0	0	0	0	0

Mean	193.86	637	1.198	35.10	1931.968
Std. Deviation	51.99	406	0.455	6.00	1261.449
Variance	2698.71	164350	0.207	35.93	1588447.707
Minimum	74	26	0.159	19.4	79.000
Maximum	306	2496	3.445	56.5	6741.000

There are special diagrams that make it easier to check the normality of data distribution. One of these graphs is the normal probability plot. For each data value, the graph shows the observed value (*X* axis) and the percentage of the expected value (when the sample data has a normal distribution) (*Y* axis) (Fig. 3). In the following, the input variables and output variable are described: this figure show that T (~ 10% not normal), API (~ 20% not normal) and BPP (~ 10% not normal) are a normal distribution but γ_g (~ 70% not normal) and Rs (~ 40% not normal) are not normal distribution. This figure shows the mean, Stdv, N, AD and P-value for each variable too.

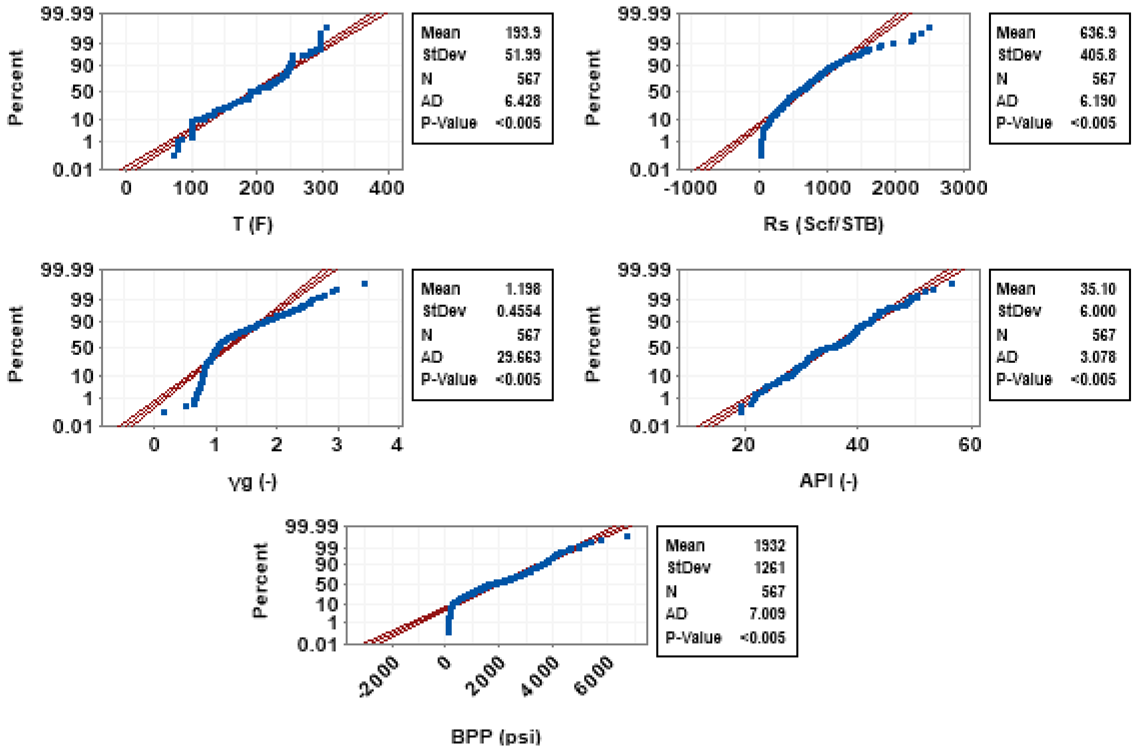

Fig. 3. Probability plot of the variables displayed are: temperature (*T*), solution gas oil ratio (R_s), Gas Specific Gravity (γ_g) and API and bubble point pressure (BPP)

Based on Fig. 4, input variables T and API are normal distribution, but the other input variables (R_s and γ_g) and output (BPP) are not normal. This figure also shows approximately what data index of the variable has amount content.

Performance accuracy assessment of the two-hybrid machine-learning-optimization algorithms and other empirical equations is computational errors between measured and predicted BPP. The statistical measures of prediction accuracy used are percentage deviation (PDi), average percentage deviation (APD), average absolute percentage deviation (AAPD), standard deviation (SD), mean squared error (MSE), root-mean-square error (RMSE), and coefficient of determination (R^2). The computation formulas for the statistical accuracy measures used are expressed in Eq. 9 to Eq. 16.

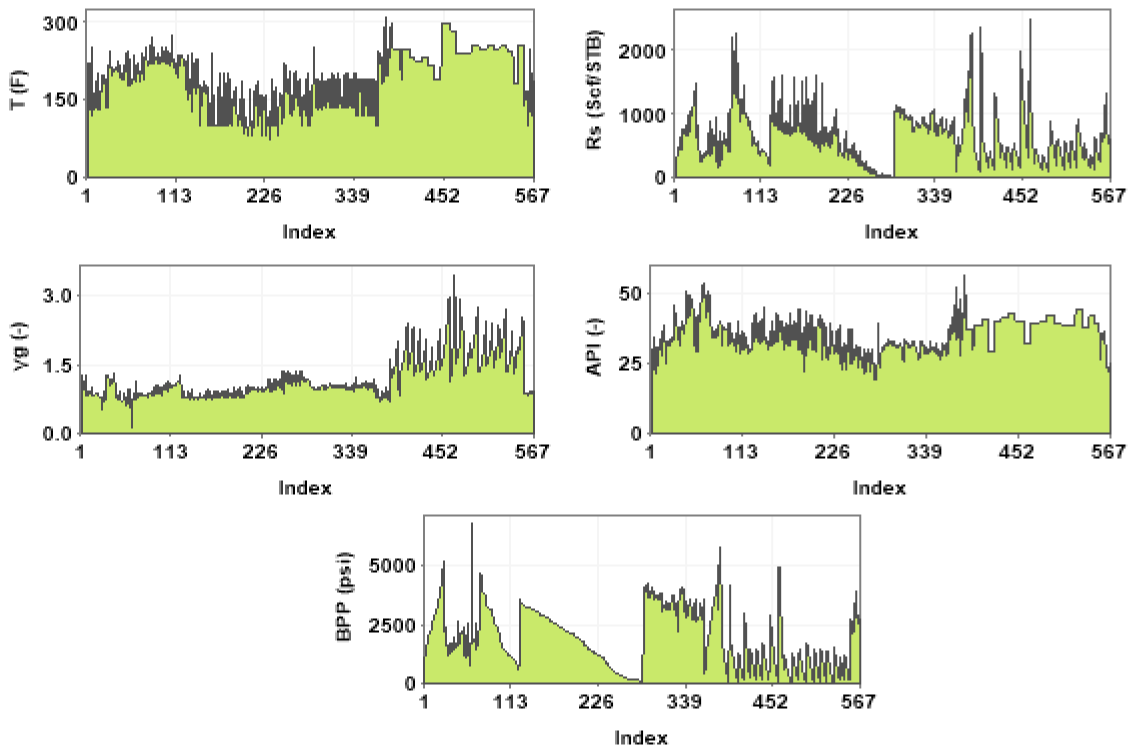

Fig. 4. Variable value versus dataset index number highlighting the ranges and extreme values associated with each variable recorded for the dataset. The variables displayed are temperature (*T*), solution gas oil ratio (R_s), Gas Specific Gravity (γ_g), API and bubble point pressure (BPP)

Percentage difference (PD_i):

$$PD_i = \frac{\xi_{(Measured)} - \xi_{(Predicted)}}{\xi_{(Measured)}} \text{ x } 100 \tag{9}$$

Average percent deviation (APD): (10)

$$APD = \frac{\sum_{i=1}^{n} PD_i}{n}$$

Absolute average percent deviation (AAPD):

$$AAPD = \frac{\sum_{i=1}^{n} |PD_i|}{n} \tag{11}$$

Standard Deviation (SD):

$$SD = \sqrt{\frac{\sum_{i=1}^{n} (D_i - Dimean)^2}{n-1}} \tag{12}$$

$$Dimean = \frac{1}{n} \sum_{i=1}^{n} \left(\xi_{Measured_i} - \xi_{Predicted_i}\right) \tag{13}$$

Mean Square Error (MSE):

$$MSE = \frac{1}{n} \sum_{i=1}^{n} \left(\xi_{Measured_i} - \xi_{Predicted_i}\right)^2 \tag{14}$$

Root Mean Square Error (RMSE):

where n is a number of data records, x_i is measured dependent variable value for the ith data record and, y_i is predicted dependent variable value for the ith data record.

$$RMSE = \sqrt{MSE} \quad = \sqrt{\frac{\sum_{i=1}^{n} (x_i - y_i)^2}{n}} \tag{15}$$

Coefficient of Determination (R^2):

$$R^2 = 1 - \frac{\sum_{i=1}^{N} (\xi_{Predicted_i} - \xi_{Measured_i})^2}{\sum_{i=1}^{N} \left(\varphi_{Predicted_i} - \frac{\sum_{I=1}^{n} \xi_{Measured_i}}{n}\right)^2} \tag{16}$$

Results and discussion

BPP is an essential parameter for the development and management of the gas and oil reservoir. However, the archive of this parameter does not have economic efficiency, so other routine parameters, including T, R_s, γ_g, and API, can be employed to predict BPP. In this study, two innovatively combined methods, DWKNN-ICA and DWKNN-GSA, are applied to determine BBP and the performance of those compared with previously developed BPP models. Tables 5 to 7 show the performance of the developed hybrid models and some equations based on five statical errors established to predict BPP. The statistical error metrics for training and testing subsets and the total data set are listed in Tables 5 to 7, respectively. Comparing the statistical metrics shown in Tables 5 to 7 demonstrates the lowest error and best accuracy of were achieved by DWKNN-ICA (the RMSE = 0.90276 psi and R^2 = 1.000 for the test dataset), while for empirical models, Standing's model had an excellent accuracy RMSE = 11.981 psi and R^2 = 0.8977.

Table 5. BPP prediction performance compared to the developed hybrid models applied to the training subset for the worldwide dataset

Performance of the developed regression models based on six statistical error metrics for BPP (Train Data)						
Authors	**APD%**	**AAPD%**	**SD**	**MSE**	**RMSE**	**R^2**
Standing	-4.123	16.830	4.093	113.701	10.663	0.8295
Glaso	4.831	21.555	14.799	128.236	11.324	0.8833
Al-Marhoun	4.831	18.083	4.800	1445.066	38.014	0.3458
Dokla & Osman	-4.531	22.312	4.500	188.302	13.722	0.7041
Macary & El-Batanony	-66.422	68.085	65.762	782.758	27.978	0.7729
Petrosky & Farshad	-37.395	90.987	37.040	1766.964	42.035	0.7408
DWKNN-GSA	0.041	0.402	0.039	1.429	1.195	0.9092
DWKNN-ICA	0.003	0.019	0.003	0.324	0.569	0.9342

Table 6. BPP prediction performance compared to the developed hybrid models to the testing subset for the worldwide dataset

Performance of the developed regression models based on six statistical error metrics for BPP (Test Data)						
Authors	**APD%**	**AAPD%**	**SD**	**MSE**	**RMSE**	**R^2**
Standing	-35.603	42.245	35.357	143.546	11.981	0.8977
Glaso	28.231	31.686	23.780	313.194	17.697	0.9284
Al-Marhoun	28.231	31.098	28.032	312.021	17.664	0.9073
Dokla & Osman	-16.567	34.034	16.459	186.712	13.664	0.8986
Macary & El-Batanony	-203.191	203.191	201.765	2895.998	53.814	0.8694
Petrosky & Farshad	12.675	76.582	12.647	1186.880	34.451	0.9250
DWKNN-GSA	0.471	1.737	0.472	1.035	1.017	0.9270
DWKNN-ICA	-0.081	0.157	0.081	0.815	0.903	0.9583

Table 7. BPP prediction performance to the developed hybrid models applied to the total subset for the worldwide dataset

Performance of the developed regression models based on six statistical error metrics for BPP (Test Data)						
Authors	**APD%**	**AAPD%**	**SD**	**MSE**	**RMSE**	**R^2**
Standing	-13.506	24.405	13.389	113.701	10.663	0.8525
Glaso	11.806	24.575	17.469	128.236	11.324	0.9051
Al-Marhoun	11.806	21.962	21.866	1445.066	38.014	0.4048
Dokla & Osman	-8.119	25.806	25.913	188.302	13.722	0.7782
Macary & El-Batanony	-107.187	108.355	106.216	782.758	27.978	0.8147
Petrosky & Farshad	-22.471	86.693	22.302	1766.964	42.035	0.8096
DWKNN-GSA	0.041	0.402	0.041	3.155	1.776	0.9181
DWKNN-ICA	0.032	0.193	0.030	0.716	0.846	0.9463

Fig. 5 reveals that the hybrid machine-learning-optimizer models evaluated, DWKNN-GSA and DWKNN-ICA, deliver accurate and credible BPP prediction for test data.

Figs. 6 and 7 show the relative deviation (%) of empirical equations and the developed hybrid models for predicted BPP. Based on these figures for empirical equations and machine hybrid models, DWKNN-ICA has a perfect accuracy that the ranges from -0.0001 < PDi < 0.00015. They are considering the results provided in Figs. 5 and 6 and Tables 5 to 7 show that the hybrid machine models have better accuracy compared to other models.

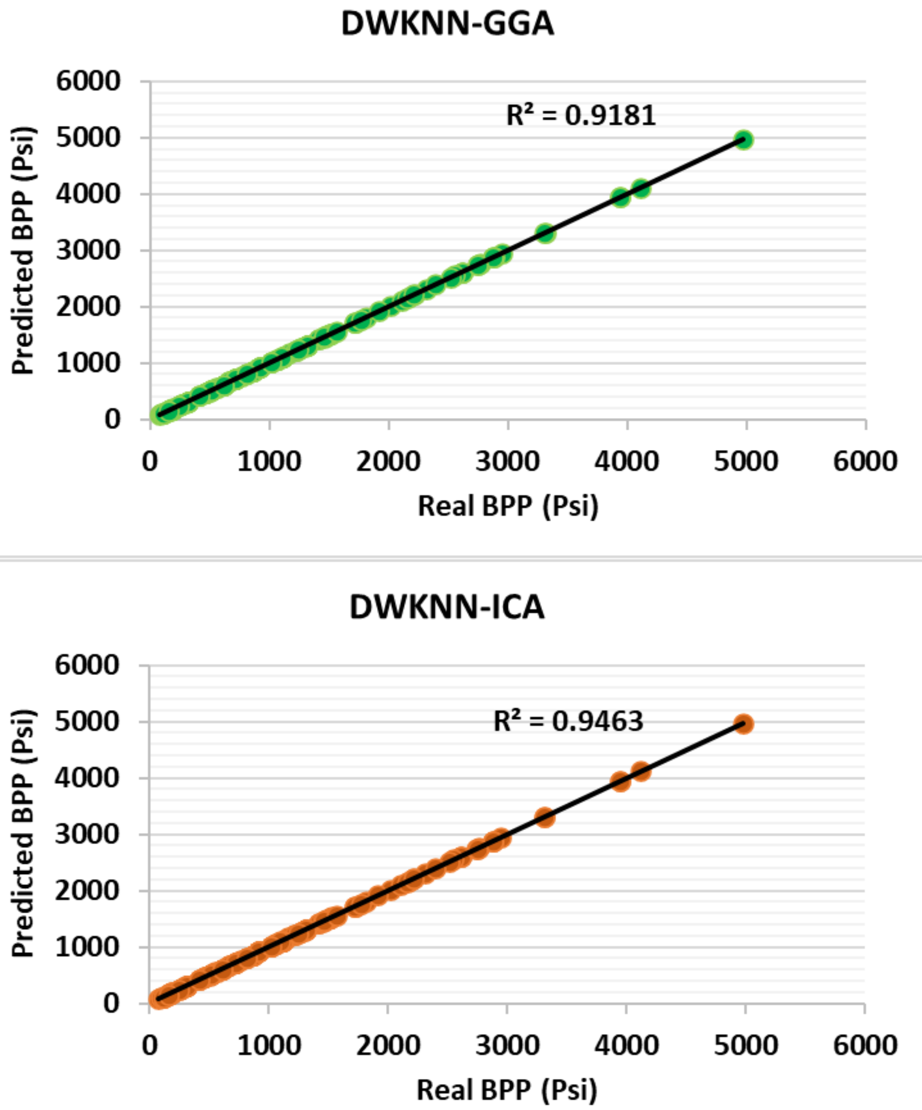

Fig. 5. Cross plot of BPP versus data index for the input variables: hybrid models (DWKNN-GSA and DWKNN-ICA) with the four independent T, R_s, γ_g and API for the worldwide sample

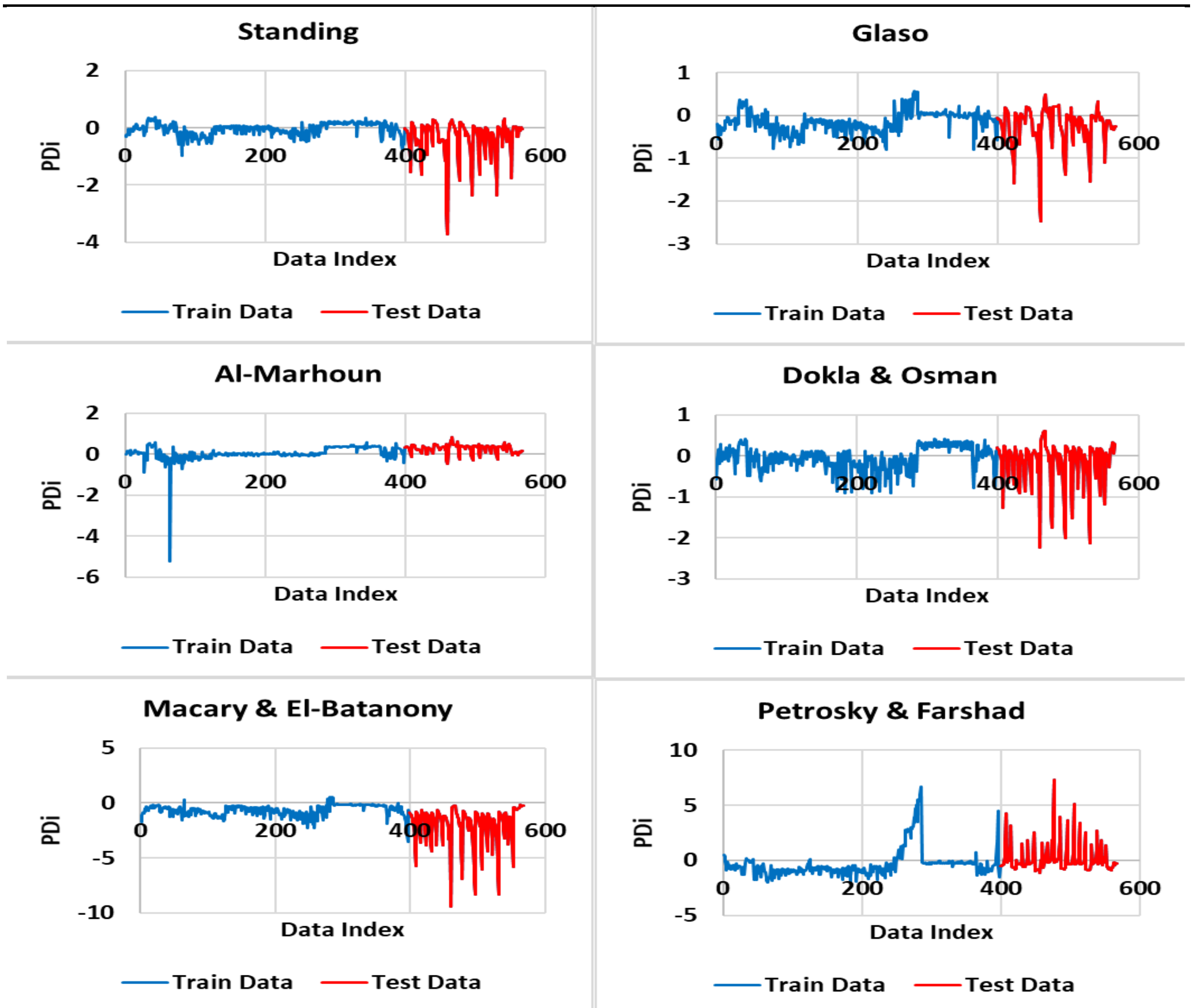

Fig. 6. Relative deviation (%) for predicted BPP values compared for all 398 training subset data records and 169 testing subset records for the empirical models evaluated

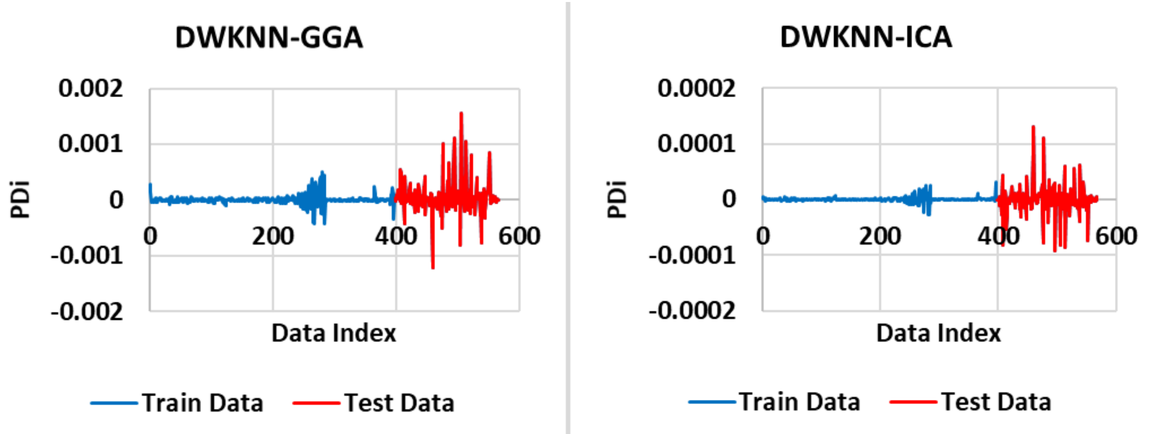

Fig. 7. Relative deviation (%) for predicted BPP values compared for all 398 training subset data records and 169 testing subset records for the two hybrid models evaluated

Iteration diagrams are used to analyze the BPP prediction as well as to reach an optimal RMSE value. As shown in this diagram, 100 iterations were used for this study (Fig. 8).

Initially, the amount of RMSE for the DWKNN-ICA model is higher than the DWKNN-GSA model. However, after iteration 40 onwards, the RMSE value of the DWKNN-ICA model becomes less than that of the DWKNN-ICA model. The comparison of RMSE for the developed models suggests that combining the ICA optimizer with DWKNN could make better and more accurate BPP predictions than the GSA optimizer.

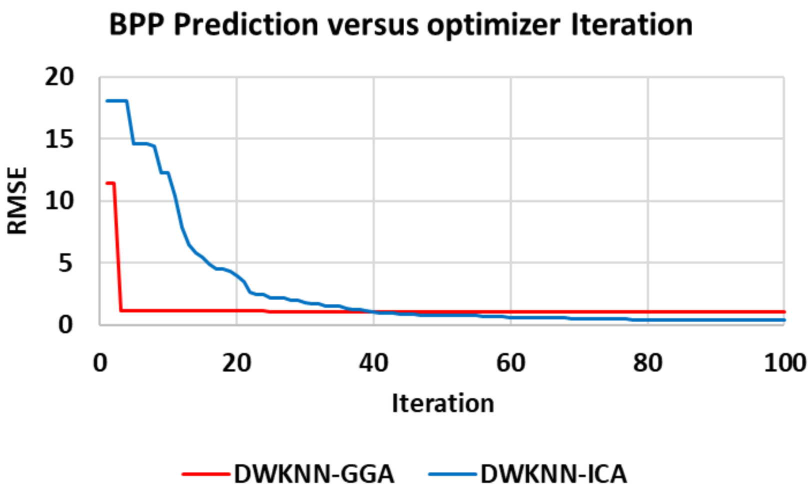

Fig. 8. Comparison of iterations for two hybrid machine-learning -optimizer methods applied to the training subsets

One of the best and most useful ways to determine each parameter's effect on the prediction model's output is Spearman's correlation. For this purpose, Eq. 17 was used to assess each of the input variables' impact on the model's output (BPP).

$$\rho = \frac{\sum_{i=1}^{n}(H_i - \bar{H})(Z_i - \bar{Z})}{\sqrt{\sum_{i=1}^{n}(H_i - H)^2 \sum_{i=1}^{n}(Z_i - \bar{Z})^2}} \tag{17}$$

where H_i is the value of data record i for input variable H, $\bar{H}$ is the average value of the input variable H, Z_i is the value of data record i for input variable Z, $\bar{Z}$ is the average of the input variable Z, and, n is the number of data points in the population.

After examining the necessary Haas on the input variables, it is determined that R_s have a positive effect, and other input variables (γ_g, T, and API) have a negative impact. The magnitude of parameters' influence, the R_s, has the highest impact on the output, while the lowest effect is for API (Fig. 9).

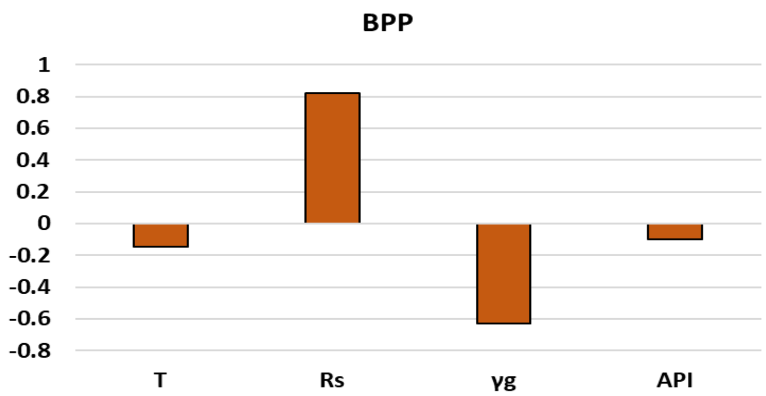

Fig. 9. Spearman's correlation coefficient for the input variable to the prediction of BPP. In terms of influence: $R_s > \gamma_g >$ T > API

Conclusion

Determining the bubble point pressure is one of the main factors in the development and progress of oil and gas reservoirs. This research uses 567 datasets from worldwide, where input variables are solution gas-oil ratio (R_s), gas specific gravity (γ_g), API gravity (API) that are readily available in the industry. The bubble point pressure, which is a key and costly parameter, is predicted by two innovative combined hybrid algorithms, which are among the latest algorithms that researchers have not yet used to predict BPP.

In this research, two novel algorithms named DWKNN-GSA and DWKNN-ICA were developed for predicting the BPP. A distinctive, unique feature of these algorithms is their high accuracy.

The best algorithm in terms of accuracy is DWKNN-ICA, where RMSE = 0.90276 psi and R2 = 1.000 for the test dataset. To compare the developed hybrid models' performance, some previously established empirical correlations were applied to the data set evaluated in this work. Among empirical models used, Standing model showed the best accuracy RMSE = 11.981 psi and R^2 = 0.8977. Comparison of the hybrid models developed with former empirical models showed that hybrid models have better performance and can predict BPP with much more accuracy than the empirical models. Moreover, Spearman's correlation coefficient assessment for the input variables demonstrated that the R_s and API have the highest and the lowest impact on the output (BPP).

Acknowledgements

The authors are grateful to Ms. Kalaei for his technical support and efforts in collecting the data needed for this study.

Nomenclature

AAPD	Absolute average percent deviation
ANN	Artificial Neural Network
APD	Average percent deviation
API	Oil density
BPP	Bubble point pressure
DWKNN	Distance-Weighted K-nearest neighbor algorithm
GORs	Solution gas oil ratio
GSA	Gravitational Search Algorithm
H_i	The value of data record i for input variable H
ICA	Imperialist Competitive Algorithm
MSE	Mean square error
n	The number of data points in the population
OFVF	Oil formation volume factor
PD_i	Percentage difference
R^2	Coefficient of determination
RMSE	Root mean square error
SD	Standard deviation
T	Temperature
Z_i	The value of data record i for input variable Z
γ_g	Gas specific gravity
$\bar{H}$	The average value of the input variable H
$\bar{Z}$	The average of the input variable Z
x_i	Measured dependent variable value for the ith data record
y_i	Predicted dependent variable value for the ith data record

μ_{OD} Dead oil viscosity

References

[1] El-Banbi A, Alzahabi A, El-Maraghi A. PVT Property Correlations: Selection and Estimation. Gulf Professional Publishing; 2018 Apr 20.

[2] Talebi R, Ghiasi MM, Talebi H, Mohammadyian M, Zendehboudi S, Arabloo M, Bahadori A. Application of soft computing approaches for modeling saturation pressure of reservoir oils. Journal of Natural Gas Science and Engineering. 2014 Sep 1;20:8-15.

[3] Macary S, El-Batanoney M. Derivation of PVT correlations for the Gulf of Suez crude oils. Journal of the Japan Petroleum Institute. 1993. 36(6):472-478.

[4] Chaudhary AS, Ehlig-Economides CA, Wattenbarger RA. Shale oil production performance from a stimulated reservoir volume. SPE Annual Technical Conference and Exhibition. 2011.

[5] Soliman AA, Attia AM, Abdelwahab MH. Development of new models for predicting crude oil bubble point pressure, oil formation volume factor, and solution gas-oil ratio using genetic algorithm. Journal of Petroleum and Mining Engineering. 2020 Dec 1;22(2):17-39.

[6] Farasat A, Shokrollahi A, Arabloo M, Gharagheizi F, Mohammadi AH. Toward an intelligent approach for determination of saturation pressure of crude oil. Fuel processing technology. 2013 Nov 1;115:201-14.

[7] Danesh A. PVT and phase behaviour of petroleum reservoir fluids. Elsevier; 1998 May 7.

[8] Hemmati MN, Kharat R. Evaluation of empirically derived PVT properties for Middle East crude oils. Scientia Iranica, 2007. 14(4): p. 358-368.

[9] Ghorbani H, Moghadasi J, Dashtbozorg A, Abarghoyi PG. The exposure of new estimating models for bubble point pressure in crude oil of one of the oil fields in Iran. American Journal of Oil and Chemical Technologies. 2017:178-93.

[10] Mohamadian N, and Ghorbani, H. An investigation on chemical formation damage in Iranian reservoir by focus on mineralogy role in shale swelling potential in Pabdeh and Gurpi formations. Advances in Environmental Biology, 2015. 9(4):161-166.

[11] Darvishpour A, Sefiabad MC, Wood DA, Ghorbani H. Wellbore stability analysis to determine the safe mud weight window for sandstone layers. Petroleum Exploration and Development, 2019. 46(5):1031-1038.

[12] Mohamadian N, Ghorbani H, Wood DA, Hormozi HK. Rheological and filtration characteristics of drilling fluids enhanced by nanoparticles with selected additives: an experimental study. Advances in Geo-Energy Research, 2018. 2(3):228-236.

[13] Ghorbani H, Moghadasi, J. Development of a New Comprehensive Model for Choke Performance Correlation in Iranian Oil Wells. Advances in Environmental Biology, 2014. 8(17): 877-882.

[14] Ghorbani H, Moghadasi J, Dashtbozorg A, Kooti, S. Developing a New Multiphase Model for Choke Function Relation for Iran's Gas Wells. American Journal of Oil and Chemical Technologies, 2017. 5(3):194-202.

[15] Ghorbani H, Moghadasi J, Mohamadian N, Mansouri Zadeh M, Hezarvand Zangeneh M, Molayi O, Kamali A. Development of a New Comprehensive Model for Choke Performance Correlation in Iranian Gas Condensate Wells. Advances in Environmental Biology, 2014. 8(17): 308-313.

[16] Mohamadian N, Ghorbani H, Wood DA, Khoshmardan MA. A hybrid nanocomposite of poly (styrene-methyl methacrylate-acrylic acid)/clay as a novel rheology-improvement additive for drilling fluids. Journal of Polymer Research, 2019. 26(2): p. 33.

[17] Ghaderi S, Haddadi SA, Davoodi S, Arjmand M. Application of sustainable saffron purple petals as an eco-friendly green additive for drilling fluids: A rheological, filtration, morphological, and corrosion inhibition study. Journal of Molecular Liquids, 2020. 315: 113707.

[18] Davoodi S, SA AR, Soleimanian A, Jahromi AF. Application of a novel acrylamide copolymer containing highly hydrophobic comonomer as filtration control and rheology modifier additive

in water-based drilling mud. Journal of Petroleum Science and Engineering. 2019 Sep 1;180:747-55.

[19] Davoodi S, SA AR, Jamshidi S, Jahromi AF. A novel field applicable mud formula with enhanced fluid loss properties in high pressure-high temperature well condition containing pistachio shell powder. Journal of Petroleum Science and Engineering. 2018 Mar 1;162:378-85.

[20] Davoodi S, SA AR, Rukavishnikov V, Minaev K. Insights into application of acorn shell powder in drilling fluid as environmentally friendly additive: filtration and rheology. International Journal of Environmental Science and Technology. 2021 Apr;18(4):835-48.

[21] Khodaeipour M, Moqadam DL, Dashtbozorg A, Ghorbani H. Nano Clay Effect on Adsorption of Benzene, Toluene and Xylene from Aqueous Solution. American Journal of Oil and Chemical Technologies: Volume. 2018 Jun;6(2).

[22] Abdali MR, Mohamadian N, Ghorbani H, Wood DA. Petroleum Well Blowouts as a Threat to Drilling Operation and Wellbore Sustainability: Causes, Prevention, Safety and Emergency Response. Journal of Construction Materials| Special Issue on Sustainable Petroleum Engineering ISSN. 2021 Feb 4;2652:3752.

[23] Hassanpouryouzband A, Yang J, Okwananke A, Burgass R, Tohidi B, Chuvilin E, Istomin V, Bukhanov B. An Experimental Investigation on the Kinetics of Integrated Methane Recovery and CO 2 Sequestration by Injection of Flue Gas into Permafrost Methane Hydrate Reservoirs. Scientific reports. 2019 Nov 7;9(1):1-9.

[24] Hassanpouryouzband A, Yang J, Tohidi B, Chuvilin E, Istomin V, Bukhanov B. Geological CO2 capture and storage with flue gas hydrate formation in frozen and unfrozen sediments: method development, real time-scale kinetic characteristics, efficiency, and clathrate structural transition. ACS Sustainable Chemistry & Engineering. 2019 Feb 15;7(5):5338-45.

[25] Hassanpouryouzband A, Yang J, Tohidi B, Chuvilin E, Istomin V, Bukhanov B, Cheremisin A. CO2 capture by injection of flue gas or CO2–N2 mixtures into hydrate reservoirs: Dependence of CO2 capture efficiency on gas hydrate reservoir conditions. Environmental science & technology. 2018 Mar 7;52(7):4324-30.

[26] Hassanpouryouzband A, Yang J, Tohidi B, Chuvilin E, Istomin V, Bukhanov B, Cheremisin A. Insights into CO2 capture by flue gas hydrate formation: gas composition evolution in systems containing gas hydrates and gas mixtures at stable pressures. ACS Sustainable Chemistry & Engineering. 2018 Mar 28;6(5):5732-6.

[27] Hassanpouryouzband A, Farahani MV, Yang J, Tohidi B, Chuvilin E, Istomin V, Bukhanov B. Solubility of flue gas or carbon dioxide-nitrogen gas mixtures in water and aqueous solutions of salts: Experimental measurement and thermodynamic modeling. Industrial & Engineering Chemistry Research. 2019 Jan 23;58(8):3377-94.

[28] Hassanpouryouzband A, Joonaki E, Farahani MV, Takeya S, Ruppel C, Yang J, English NJ, Schicks JM, Edlmann K, Mehrabian H. Gas hydrates in sustainable chemistry. Chemical Society Reviews, 2020. 49(15):5225-5309.

[29] Hassanpouryouzband A, Joonaki E, Edlmann K, Heinemann N, Yang J. Thermodynamic and transport properties of hydrogen containing streams. Scientific Data. 2020 Jul 9;7(1):1-4.

[30] Hassanpouryouzband A, Joonaki E, Taghikhani V, Bozorgmehry Boozarjomehry R, Chapoy A, Tohidi B. New two-dimensional particle-scale model to simulate asphaltene deposition in wellbores and pipelines. Energy & Fuels. 2017 Nov 9;32(3):2661-72.

[31] Rashaid M, Harrison C, Ayyad H, Dumont H, Smythe E, Sullivan M, Meier J, Fukagawa S, Miyashita M, Grant B, Morikami Y. A downhole wireline module for the measurement of bubble point pressure. InAbu Dhabi International Petroleum Exhibition & Conference 2019 Nov 11. OnePetro.

[32] Ahmadi MA, Zendehboudi S, James LA, Elkamel A, Dusseault M, Chatzis I, Lohi A. New tools to determine bubble point pressure of crude oils: Experimental and modeling study. Journal of Petroleum Science and Engineering. 2014 Nov 1;123:207-16.

[33] Yang G, Fan Z, Li X. Determination of confined fluid phase behavior using extended Peng-Robinson equation of state. Chemical Engineering Journal. 2019 Dec 15;378:122032.

[34] Standing MB. A pressure-volume-temperature correlation for mixtures of California oils and gases. InDrilling and Production Practice 1947 Jan 1. OnePetro.

[35] Glaso O. Generalized pressure-volume-temperature correlations. Journal of Petroleum Technology. 1980 May 1;32(05):785-95.

[36] Al-Marhoun MA. PVT correlations for Middle East crude oils. Journal of Petroleum Technology. 1988 May 1;40(05):650-66.

[37] Dokla M, Osman M. Correlation of PVT Properties for UAE Crudes (includes associated papers 26135 and 26316). SPE formation evaluation. 1992 Mar 1;7(01):41-6.

[38] Petrosky GE, Farshad FF. Pressure-volume-temperature correlations for Gulf of Mexico crude oils. InSPE annual technical conference and exhibition 1993 Oct 3. OnePetro.

[39] Ghiasi MM, Shahdi A, Barati P, Arabloo M. Robust modeling approach for estimation of compressibility factor in retrograde gas condensate systems. Industrial & Engineering Chemistry Research. 2014 Aug 13;53(32):12872-87.

[40] Arabloo M, Shokrollahi A, Gharagheizi F, Mohammadi AH. Toward a predictive model for estimating dew point pressure in gas condensate systems. Fuel processing technology. 2013 Dec 1;116:317-24.

[41] Bandyopadhyay P, Sharma A. Development of a new semi analytical model for prediction of bubble point pressure of crude oils. Journal of Petroleum Science and Engineering. 2011 Sep 1;78(3-4):719-31.

[42] El-Sebakhy EA. Forecasting PVT properties of crude oil systems based on support vector machines modeling scheme. Journal of Petroleum Science and Engineering. 2009 Feb 1;64(1-4):25-34.

[43] Gharbi RB. Elsharkawy AM, Karkoub M. Universal neural-network-based model for estimating the PVT properties of crude oil systems. Energy, 1999. 13(2):454-458.

[44] Boukadi F, Al-Alawi S, Al-Beman, A, Al-Qassabi S. Establishing PVT correlations for Omani oils. Petroleum science and technology, 1999. 17(5-6:637-662.

[45] Al-Marhoun MA, Osman EA. Using artificial neural networks to develop new PVT correlations for Saudi crude oils. InAbu Dhabi international petroleum exhibition and conference 2002 Oct 13. OnePetro.

[46] Rafiee-Taghanaki S, Arabloo M, Chamkalani A, Amani M, Zargari MH, Adelzadeh MR. Implementation of SVM framework to estimate PVT properties of reservoir oil. Fluid Phase Equilibria. 2013 May 25;346:25-32.

[47] Salehinia S, Salehinia Y, Alimadadi F, Sadati SH. Forecasting density, oil formation volume factor and bubble point pressure of crude oil systems based on nonlinear system identification approach. Journal of Petroleum Science and Engineering. 2016 Nov 1;147:47-55.

[48] Seyyedattar M, Ghiasi MM, Zendehboudi S, Butt S. Determination of bubble point pressure and oil formation volume factor: Extra trees compared with LSSVM-CSA hybrid and ANFIS models. Fuel. 2020 Jun 1;269:116834.

[49] Ghorbani H, Wood DA, Choubineh A, Mohamadian N, Tatar A, Farhangian H, Nikooey A. Performance comparison of bubble point pressure from oil PVT data: Several neurocomputing techniques compared. Experimental and Computational Multiphase Flow. 2020 Dec;2(4):225-46.

[50] Shokrollahi A, Tatar A, Safari H. On accurate determination of PVT properties in crude oil systems: Committee machine intelligent system modeling approach. Journal of the Taiwan Institute of Chemical Engineers. 2015 Oct 1;55:17-26.

[51] Moradi B, Malekzadeh E, Amani M, Boukadi FH, Kharrat R. Bubble point pressure empirical correlation. InTrinidad and Tobago Energy Resources Conference 2010 Jan 1. Society of Petroleum Engineers.

[52] Rashidi S, Mehrad M, Ghorbani H, Wood DA, Mohamadian N, Moghadasi J, Davoodi S. Determination of bubble point pressure & oil formation volume factor of crude oils applying multiple hidden layers extreme learning machine algorithms. Journal of Petroleum Science and Engineering. 2021 Jul 1;202:108425.

[53] Barjouei HS, Ghorbani H, Mohamadian N, Wood DA, Davoodi S, Moghadasi J, Saberi H. Prediction performance advantages of deep machine learning algorithms for two-phase flow rates through wellhead chokes. Journal of Petroleum Exploration and Production. 2021 Mar;11(3):1233-61.

[54] Choubineh A, Ghorbani H, Wood DA, Moosavi SR, Khalafi E, Sadatshojaei E. Improved predictions of wellhead choke liquid critical-flow rates: modelling based on hybrid neural network training learning based optimization. Fuel. 2017 Nov 1;207:547-60.

[55] Ghorbani H, Moghadasi J, Wood DA. Prediction of gas flow rates from gas condensate reservoirs through wellhead chokes using a firefly optimization algorithm. Journal of Natural Gas Science and Engineering. 2017 Sep 1;45:256-71.

[56] Ghorbani H, Wood DA, Moghadasi J, Choubineh A, Abdizadeh P, Mohamadian N. Predicting liquid flow-rate performance through wellhead chokes with genetic and solver optimizers: an oil field case study. Journal of Petroleum Exploration and Production Technology. 2019 Jun;9(2):1355-73.

[57] Ghorbani H, Wood DA, Mohamadian N, Rashidi S, Davoodi S, Soleimanian A, Shahvand AK, Mehrad M. Adaptive neuro-fuzzy algorithm applied to predict and control multi-phase flow rates through wellhead chokes. Flow Measurement and Instrumentation. 2020 Dec 1;76:101849.

[58] Farsi M, Mohamadian N, Ghorbani H, Wood DA, Davoodi S, Moghadasi J, Alvar MA. Predicting Formation Pore-Pressure from Well-Log Data with Hybrid Machine-Learning Optimization Algorithms. Natural Resources Research. 2021 Apr 1:1-27.

[59] Hazbeh O, Aghdam SK, Ghorbani H, Mohamadian N, Alvar MA, Moghadasi J. Comparison of accuracy and computational performance between the machine learning algorithms for rate of penetration in directional drilling well. Petroleum Research. 2021 Mar 2.

[60] Mohamadian N, Ghorbani H, Wood DA, Mehrad M, Davoodi S, Rashidi S, Soleimanian A, Shahvand AK. A geomechanical approach to casing collapse prediction in oil and gas wells aided by machine learning. Journal of Petroleum Science and Engineering. 2021 Jan 1;196:107811.

[61] Rashidi S, Mohamadian N, Ghorbani H, Wood DA, Shahbazi K, Alvar MA. Shear modulus prediction of embedded pressurized salt layers and pinpointing zones at risk of casing collapse in oil and gas wells. Journal of Applied Geophysics. 2020 Dec 1;183:104205.

[62] Farsi M, Barjouei HS, Wood DA, Ghorbani H, Mohamadian N, Davoodi S, Nasriani HR, Alvar MA. Prediction of oil flow rate through orifice flow meters: Optimized machine-learning techniques. Measurement. 2021 Apr 1;174:108943.

[63] Ghorbani H, Wood DA, Choubineh A, Tatar A, Abarghoyi PG, Madani M, Mohamadian N. Prediction of oil flow rate through an orifice flow meter: Artificial intelligence alternatives compared. Petroleum. 2020 Dec 1;6(4):404-14.

[64] Ranaee E, Ghorbani H, Keshavarzian S, Abarghoei PG, Riva M, Inzoli F, Guadagnini A. Analysis of the performance of a crude-oil desalting system based on historical data. Fuel. 2021 May 1;291:120046.

[65] Li D, Zhang B, Li C. A feature-scaling-based $ k $-nearest neighbor algorithm for indoor positioning systems. IEEE Internet of Things Journal. 2015 Oct 27;3(4):590-7.

[66] Gholoobi A, Stavrou S. RSS based localization using a new WKNN approach. In2015 7th International Conference on Computational Intelligence, Communication Systems and Networks 2015 Jun 3 (pp. 27-30). IEEE.

[67] Rashedi E, Nezamabadi-Pour H, Saryazdi S. GSA: a gravitational search algorithm. Information sciences. 2009 Jun 13;179(13):2232-48.

[68] Hu H, Cui X, Bai Y. Two kinds of classifications based on improved gravitational search algorithm and particle swarm optimization algorithm. Advances in Mathematical Physics. 2017 Sep 11;2017.

[69] Naveshki M, Naghiei A, Soltani Tehrani P, Ahmadi Alvar M, Ghorbani H, Mohamadian N, Moghadasi J. Prediction of bubble point pressure using new hybrid computationail intelligence models. Journal of Chemical and Petroleum Engineering. 2021 Jun 30.

[70] Pan Z, Lei D, Zhang Q. A new imperialist competitive algorithm for multiobjective low carbon parallel machines scheduling. Mathematical problems in engineering. 2018 Apr 16;2018.

[71] Abdi B, Mozafari H, Ayob A, Kohandel R. Imperialist competitive algorithm and its application in optimization of laminated composite structures. European Journal of Scientific Research. 2011 Jan 1;55(2):174-87.

How to cite: M Naveshki , Naghiei A, Soltani-Tehrani P, Ahmadi-Alvar M, Ghorbani H, Mohamadian N, Moghadasi J. Prediction of Bubble Point Pressure using New Hybrid Computational Intelligence Models. *Journal of Chemical and Petroleum Engineering*. 2021; 55(2): 203- 222.